Current Medical Imaging Reviews, 2017, *13*, 89-98

RESEARCH ARTICLE

Decision Support System for Lymphoma Classification

Ahmed E-S. Negm[a,*], Ahmed H. Kandil[a,b] and Osama A. E-F. Hassan[a,c]

[a]*Systems and Biomedical Engineering Department, High Institutes of Engineering, Al Shorouk Academy, Al Shorouk city, Cairo, Egypt;* [b]*Systems and Biomedical Engineering Department, Faculty of Engineering, Cairo University, Giza, Egypt;* [c]*Professor Doctor Expert of Histopathology and Electron Microscopy Services / Central Medical and Research Laboratories / Egyptian Armed Forces, and International Medical Centre "IMC" Cairo, Egypt*

ARTICLE HISTORY

Received: August 17, 2015
Revised: April 07, 2016
Accepted: April 08, 2016

DOI:
10.2174/1573405612666160519124752

Abstract: The diffuse lymphoma is a malignant tumor of lymphoid tissues. It is associated with abnormal, unlimited and uncontrolled proliferation of lymphoid cells. Until now, expert pathologists have identified diffuse lymphoma cells disease manually. This paper introduces automatic system with a friendly user interface to differentiate between the categories of the diffuse lymphoma cells. This research is based on the morphological features such as size, perimeter and circularity. The cell size is a critical element in the classification of diffuse lymphoma according to international formulation standards. Therefore, the applied procedures identify lymphoid cell population in digital microscopic images.

The cells are classified using their morphological data according to the characteristics of each cell such as: circularity, perimeter, area, and color density. The number of cells is taken into consideration in the developed approach. Image processing techniques are applied to digital microscopic images to measure morphological parameters and to overcome image problems such as overlapping and cell distortion that affect the sensitivity of the measured data. The developed procedures help the pathologists to come to a decision regarding the classification of diffuse lymphoma. Moreover, it can be used to train medical students and young pathologists.

Keywords: Decision Support System, Diffuse lymphoma, Morphology, Image processing.

1. INTRODUCTION

The subject of this research is within the domain of morphometric analysis of digital microscopic images. Digital microscopic images are good enough in revealing morphological details allowing analytic techniques to be applied for making cell features measurements. The cell size is one of the most important features used in classification of the diffuse lymphoma class which affects the pre-treatment planning [1, 2]. Cell size is a critical element in classification of diffuse lymphoma.

Pathologists tend to classify diffuse lymphoma subjectively based on their experience. The need for qualitative assessment developed by a group of local expert pathologists, in an attempt to solve related problems as possible overlap (mixed small and large diffuse lymphoma) becomes necessary as shown in (Fig. **1**). The classification according to size is a critical parameter in diffuse lymphoma diagnosis and management as in a revised European-American classification of lymphoid neoplasms.

The domain of morphometric analysis is used for more accurate assessment of cellular features, histologic pattern changes in tissue and cellular preparations. Further, it is used for studying subcellular features particularly in studying the effect of pharmaceutical preparations, drugs and toxins. Other approaches depending on the analysis of DNA and hormone receptors related to tumor research were also studied intensively [3]. Automated analytical systems became available for research and diagnosis [3, 4].

In principle, the characteristics of the microscopic image may be identified by automatic, semi-automatic or manual techniques [5]. Geometric and texture features are extracted from the input image for identification and classification. Important geometric features like area, bounding box, convex area, perimeter, major-axis, minor-axis and solidity are extracted [6]. Regarding texture feature extraction, Gabor is one of the most important methods for texture features extraction [7, 8]. Image texture is a function of homogeneity, roughness, smoothness, coarseness, *etc.* Fourier filters are used for extracting entropy, homogeneity, contrast, and spatial frequency [6].

Image processing techniques are applied for studying problems related to image segmentation. Knowledge-based, level set and snake-driven segmentation approaches are explored in medical imaging [9, 10]. Using segmentation to obtain visual features for content-based medical image retrieval, depends on many features such as structural using convolution filters, textural using co-occurrence matrix, Gabor filter, localization using edge detectors, and color fea-

*Address correspondence to this author at the Systems and Biomedical Engineering Department, High Institutes of Engineering, Al Shorouk Academy, Al Shorouk city, Cairo, Egypt; Tel: +20226300041 / +201220655595; Fax: +20226300041; E-mail: a.negm@sha.edu.eg

tures using 64 different colors. Jaakko Laitakari and Yayun Zhou relied on hysteresis thresholding for nuclei segmentation. They developed a cell nuclei segmentation algorithm. The basic steps of the algorithm are color space decomposition, morphologic reconstruction, hysteresis thresholding and post processing. The output of the algorithm identifies the cell nuclei and delineates the boundaries of nuclei [11, 12].

Level set representations are emerging techniques to represent shapes and track moving interfaces for segmentation and tracking [13-16]. According to R. Malladi *et al*., region growing algorithm has been applied to segment image based on color, size, shape, texture, orientation, and border features. Peter Howarth et.al performed a background subtraction to enhance segmentation results [17]. José Crespo del Arco *et al*., [18] stated that watershed segmentation has been used with level set to segment gray level MRI images. The smoothed image is enhanced using edge enhancing filter and then the result is passed to Watershed segmentation module to detect regions that are enhanced using level set. Q. Chen *et al.* [19] pointed out that the watershed combined with distance transform "Chessboard" gives good result in segmentation.

A.Sai Prasad *et al*., obatined separated images of individual cells and used watershed for separating the clumped cells [20]. The performance of the method is evaluated by comparing the automatically extracted blood particles with manual segmentations. Chessboard distance transform function segments almost all the clumped cells.

Overlapping and clustering are major problems that should be resolved by the algorithm for separation. The automated count is based on separating the overlapping with the watershed algorithm. Morphological operations preserve the essential shapes of the objects and removal of noise [21]. Dougherty *et al*. [22] introduced the application of structured elements to an image by morphological operators based on shape characteristics. Structure elements and set operator are morphological operators. Objects in the input image are processed according to the shape characteristics encoded in the structuring element. Structuring element and the applied set operator define the morphological operator.

H.B.Kekre *et al*. [23, 24] used morphological operations and median filters in noise removal and in separating the objects. The algorithm was tested on 115 microscopic images of size 256x256 and succeeded with specificity of 90% and sensitivity of 60% to detect abnormal white blood cells.

Successful automatic and semi-automatic techniques have been applied for identification of acute leukemia cells [25]. A number of recent studies have been applied to Lymphoma and Leukemia with different staining to assess morphological analysis of cells [26-28]. A. Negm *et al*. [29] presented segmentation of the Blast cells in leukemia images. They developed an algorithm able to identify the Blast cells under specified criteria of image processing and enhancement. The algorithm consists of panel selection followed by segmentation using K-means clustering followed by refinement process. Their data set consists of 757 images with overall sensitivity of 99.348%, specificity of 99.529%, and accuracy of 99.517%. According to Schmitz *et al.* [28], Lymphoma is an unusual type of cancer, arising from malignant B-cells. This selection has been carried out by pathologists of 170 images.

Generally, our suggested classification system of Lymphoma is shown in (Fig. **2**). Standard pre-processing methods like Gaussian filtering, application of a threshold for background elimination and region labeling for identification of relevant tissue patches were applied [28]. For each pixel, a set of descriptors is computed as signature. The application of the minimum distance transform, for each pixel, result in one mean descriptor help in segmentation. Supervised classification assigns each pixel to the corresponding pixel class. For each pixel class, the relative fraction of pixels belonging to the respective class is computed [28].

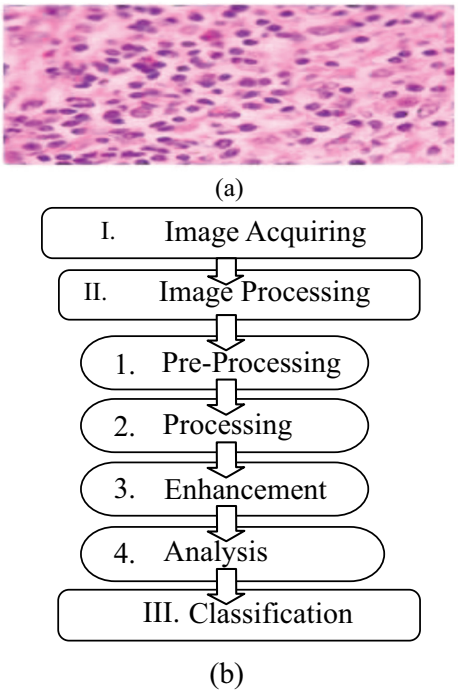

Fig. (1). Sequence of Decision making with microscopic images.

The aim of our research in this paper is to identify lymphoma cells from digital microscopic images. Morphological features of diffuse lymphoma cells were assessed and the cells were classified accordingly. This paper is organized as follows. Section 2 includes the materials and methods, which introduces the proposed segmentation algorithm. In section 3, results obtained by the proposed algorithm are presented. In section 4, discussion is presented and finally, conclusions are drawn in section 5.

2. MATERIALS AND METHODS

Materials

The data sets considered in this work were from light microscope supported with digital camera. These digital microscopic images acquired using "Axiostar plus" from Zeiss, Digital camera using Cannon Power Shot A620 with 1- 4x optical zoom And 7.1 Mega Pixels.

Tissue sections were stained by haematoxytion and Eosin. There were 360 images of diffuse lymphoma cells selected by an expert pathologist. With a resolution of 553*425

pixels, each image was processed using Laptop with 2 Microprocessor (Centrino Mobile Technology), 1GB RAM and 256MB Vega with Operating system Microsoft Window XP and Programming language MATLAB 7.

Methods

Preprocessing

The objective is to get digital images of tissue "diffuse lymphoma" previously described to extract morphological data such as the number of cells and assess characteristics of those cells such as Circularity, Perimeter, Area and the color density. Many different steps were designed to satisfy the objectives as shown in (Fig. **2**). Each step will be discussed in some detail.

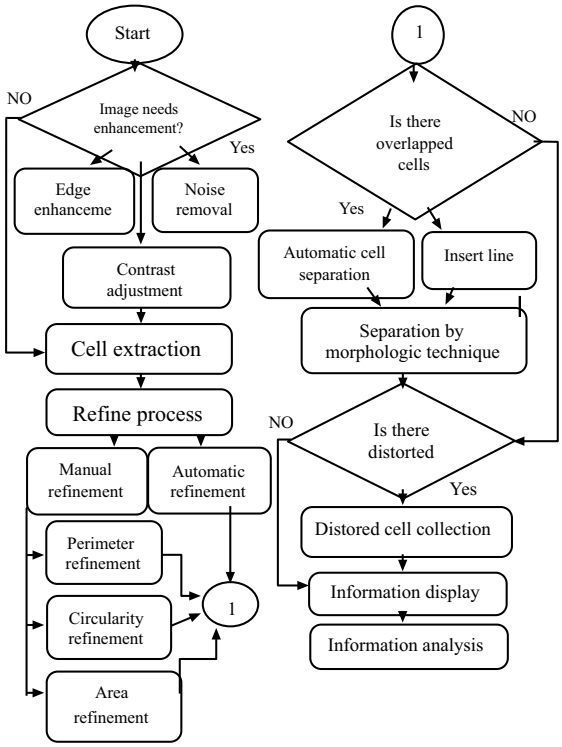

Fig. (2). Flowchart of thee decision making.

Enhancement Processing

Image quality is enhanced by applying different types of filters in various ways [30]. In our cases, this step is critical and affects other processing steps. This is clearly found in large cells, representing a problem of cell edges which are not fully connected. The degree of cytoplasm color is the same as the back ground color. It is required to be reduced by edge enhancement in the proposed system. Thus, enhancement of the edges is needed.

◊ *Edge Enhancement*

There are many different kinds of edge enhancement filters and we have chosen Prewitt filter [31]. The segmentation results are shown in (Fig. **3a**, **b**).

Prewitt Filter

An image has been created and edge changes highlighted by the filter. We used 3 x 3 filter size. Perwitt gradient value

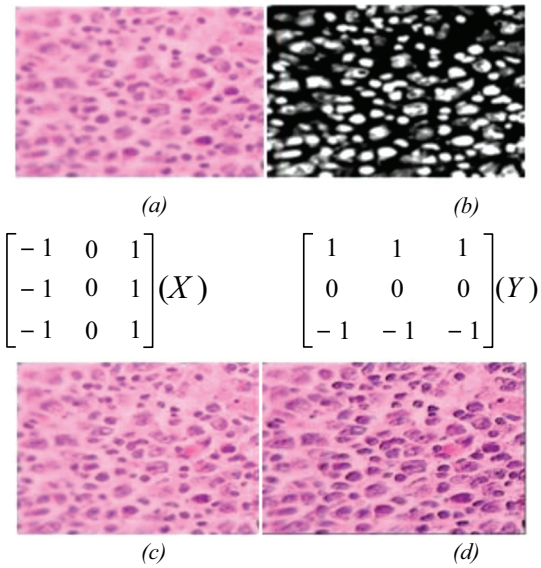

Fig. (3). (a, b) shows Effected of segmentation on the cells that have the same color degrees. (c, d) shows effect of the filter on the image for edge improvement before segmentation.

was calculated by the following templates *X, Y* in (Fig. **3c**, **d**).

Segmentation

An image pixel was partitioned into multiple pixel regions and was simplified for more valuable and easier analysis of segmentation. Our algorithm suggests minimum variance quantization technique for segmentation. It groups the pixels based on the variance between the pixel values. The pixel boxes that divide the color cube of the image vary in size. Boxes numbers, n, are used by rgb2ind function to determine and analyze the color data in the image. *i.e.* the image is partitioned into n optimally located boxes. Within each box, the pixel values are mapped to the center of the box as in uniform quantization. The resulting color map usually has the number of entries specified [32].

The manual color range selection user is prompted for feeding range of colors in the different color bands. Colors within these ranges are object pixels and other colors are considered background.

Segmentation Enhancement

Often the results of segmentation may result in over segmented objects that have to be removed. We made use of different criteria to enhance the segmentation results.

Manual Enhancement as circularity is known to be in the range of 1.3 to 0.7. The user has to define and feed in the system the range allowed for perimeter and area. Automatic enhancement is based on area threshold. In preliminary study, we defined area to be greater than 30 pixels. Object with area less than this threshold value was considered as background. The outcome of enhancement process points to specific problems that need to be dealt with, namely:-

- Cell overlap
- Cell distortion

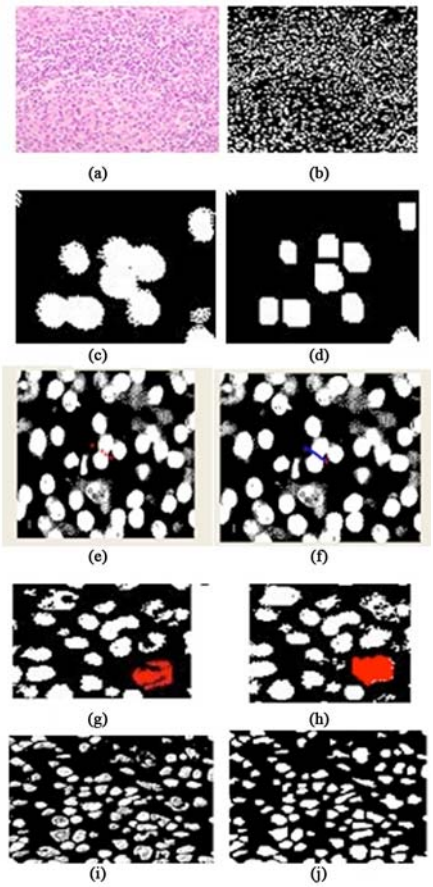

Fig. (4). The segmented image by minimum variance quantization, (c, d) The results of automatic cutter, (e, f) Overlap between cells and how user can separate them by the line that drawn between.

Overlapping Cell Separation

In some cases, some cells may overlap other cells. Therefore counting overlapped objects as a single object leads to errors in measurements and statistics. In the system we handle this problem by the following methods:

- Watershed distance segmentation [18-20, 33, and 34].
- Manual cell separation.
- Separation by morphology method [21, 22, 24, 26 and 35].

Watershed distance segmentation is this method automatically splits overlapped objects at the weakest points. Manual cell separation method is used to enter a set of points on the boundary where the program should split. These points are fitted to a curve of the third order to determine the curve points where to cut to separate the overlapped cells. The fitting is performed using polynomial regression and least squares method. Separation by morphology method is morphological opening.

Distributed Object Point Collection

Point collection is performed if the object is too hollow and/or has many distributed points. It is based on morphological operators, Dilation and Erosion. Refilling object gaps *i.e.* a gap inside the object, is recognized by the Euler number for this sub image containing the cell shown (Fig. **4**).

Region of Interest Selection

The user can focus interest on an elliptic area by any orientation using manual selection. After region selection, the user has to decide to focus on the inside area or the outside area. Program functions can be applied on the highlighted area [30]. x', y' are the coordinates of new image which are produced from experience geometric distortion x, y pixel coordinates (Fig. **5**):

$$x' = r(x, y)$$
$$y' = s(x, y) \quad (1)$$

Where r and s are functions relying upon x and y.

Assume

$$r(x, y) = \frac{r}{2}, s(x, y) = \frac{r}{2} \quad (2)$$

This halves the size of the image. This transformation can be represented using a matrix equation

$$\begin{bmatrix} x' \\ y' \end{bmatrix} = \begin{bmatrix} \frac{1}{2} & 0 \\ 0 & \frac{1}{2} \end{bmatrix} \begin{bmatrix} x \\ y \end{bmatrix} \quad (3)$$

To perform rotation of angel θ the following operation is used.

$$\begin{bmatrix} x' \\ y' \end{bmatrix} = \begin{bmatrix} \cos\theta & -\sin\theta \\ \sin\theta & \cos\theta \end{bmatrix} \begin{bmatrix} x \\ y \end{bmatrix} \quad (4)$$

The starting point of the image is generally the upper left hand corner. To rotate about the Centre, one needs to do a transformation of the origin to the Centre of the image first.

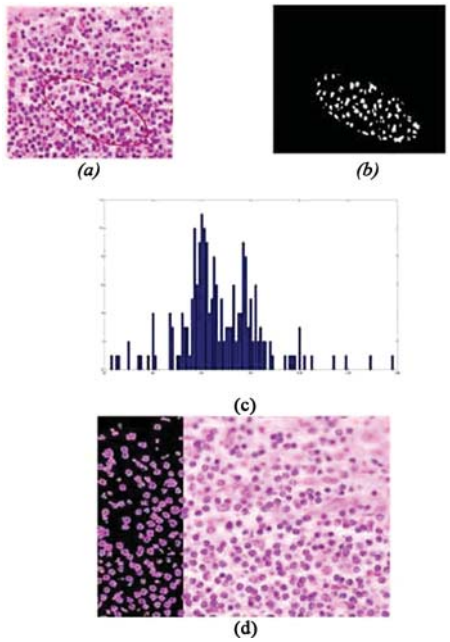

Fig. (5). (a, b) Rotated ellipse inside selection, (c) Perimeter frequency and (d) Two images sliding over each other.

Table 1. Difference between the number of cells in the image extracted by expert and the number of cells that extracted by the applied procedure.

No. of Observation Slide	No of Cells in the Field by Exp	No of Cell Extracted by Applied Procedure	Relative Error	Relative Error After Applied Procedure
1	91	80	- 12.1%	0%
2	151	106	-29.9%	0%
3	19	17	-10.6%	0%
4	33	35	+6.06%	0%
5	179	108	-39.67%	0%
6	97	113	+16.49%	0%
7	48	52	+8.33%	0%
8	43	55	+27.9%	0%
9	134	146	+8.9%	0%
10	175	85	-51.5%	0%
11	137	132	-3.65%	0%
12	90	92	+2.2%	0%

Information Displaying

Different methods are employed to display and extract information as Circularity, Area, Perimeter, Compactness and color density in pixel value [22]. The information obtained is exported to an excel sheet for further analysis. The analyzed information is uniformly quantized and displayed as frequencies on different graphs for each property.

The performance evaluation is based on expert reference images. The output images resulting from the system are matched to these reference images using the Overlay tool in the system. Sensitivity test in this research was applied by two methods. First, based on the ability of system identifying the objects in images and second, those identified by expert as shown in Table **1**. The test shows relative error with +Ve and -Ve values. These errors are caused due to overlapping of cells and the system counts these cells as one object whereas the distorted cell system counts it as more than one although it is one.

The Evaluation is repeated after enhancing the segmentation errors in the image. The outcome of sensitivity test is usually revealed as either –Ve (due to cell overlap) or +Ve (cell distortion). Either type of error totally disappeared after applying the whole steps of the algorithm as shown in Table **1**.

In this work, an algorithm was implemented for successful detection of cells. The accuracy of this algorithm was evaluated carefully to estimate its performance in real life. The specificity and sensitivity of this method were calculated using the following formula: [36]

$$\text{Sensitivity}=TP / (TP+FN) = 1 - \text{FP rate} \quad (5)$$

$$\text{FP rate} = FP / N \quad (6)$$

$$\text{Specificity}=TN/ (TN+FP) \quad (7)$$

Where True Positive (TP) is the number of cells correctly identified as cells by the algorithm of segmentation; True Negative (TN) is the number of the cells correctly identified as not cells (It represents the error of adherent cells recognized as one by the system and not as multiple cells.); False Positive (FP) is the number of cells identified as cells by the algorithm, but they are not (It represents an error due to deformed cells appearing as more than a single cell.); False Negative (FN) is the number of cells identified as not cells by the Algorithm, but they are not [37-39].

Table **2** presents a confusion matrix of the algorithm that shows 1021 true positive segmented cells. Considering the sensitivity of the algorithm is 100 % and specificity 82.35%,

The overall accuracy is calculated by

$$= (TN + TP)/ (TN+TP+FN+FP) = 96.28\ \% \quad (8)$$

And Positive Predictive Value by

$$(PPV) = TP / (TP + FP) = 95.50\ \%. \quad (9)$$

After the intervention and action steps to improve segmentation output to treat problems like cells overlap and cell

Table 2. Confusion Matrix numbers of Diffuse Lymphoma cells identifications.

	Predicated Diffuse Lymphoma Cells	
Actual Stages	TRUE	FALSE
POSITIVE	1021	48
NEGATIVE	0	224
overall accuracy	96.28%	

distortion through the algorithm, sensitivity and specificity changed to 100% and 100% in sequence.

3. RESULTS

T-test was carried out on each dataset, comparing Perimeter, Area in pixel of manual and automatic procedure. Range value of both small and large cells was presented by mean value. (Fig. **6**) shows the chosen ideal small and large cells the values. Their values were used to identify the cell selected as band from the normal reactive image.

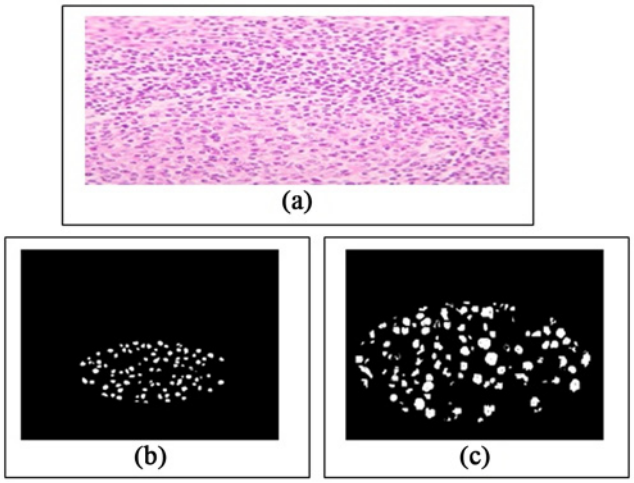

Fig. (6). Normal reactive cells, (b) Small normal cell selected by expert and (c) Large normal cells selected by expert.

The range of large lymphocytes was found to be 109 to 800 pixels and the mean was 280 pixels. The range of small lymphocytes was 56 to 280 pixels and the mean was 140 pixels. The best sequence was identified in dealing with the program in this type of image between manual and automatic methods. T- Test gives no significant difference for both population of cells shown in Tables **6, 7**. Area distribution of large reactive lymphocytes and large diffuse lymphoma cells respectively is compared to evaluate the deference between them as in Table **3**. Thus, cases of diffuse lymphoma could then be classified according to the size. Our results point to accurate differentiation between lymphoid cell classes as being large or small. The large cells were of the range 146 to 917 with the mean 521 pixels and the small cells were of the range 89 to 657 and the mean was 346 pixels shown in Tables **4**, **5**.

Comparison of the mean (area in pixels) in cases of large diffuse lymphoma cells with reactive large lymphoid cells showed a significant difference (mean value for large diffuse lymphoma cells 521 pixel and large reactive lymphoid cells 280 pixel, P-Value 6.17789E-25) as shown in Tables **3**, **4**.

Comparison of the mean (area in pixels) in cases of small diffuse lymphoma with reactive small lymphoid cells showed a significant difference (mean value for small diffuse lymphoma cells 346 pixel and small reactive lymphoid cells 140 pixel, P-Value 9.43833E-46) as in Tables **4**, **5**.

Comparison of the mean (area in pixels) in cases of small diffuse lymphoma with large diffuse lymphoma cells shown in Table **4**.

4. DISCUSSION

Since the main objective of this research was to classify diffuse lymphoma cases objectively rather than subjectively, we had to define specific limiting parameters before applying our program effectively, namely Areas and RGB. Stain-

Table 3. Comparison between Small and Large Diffuse lymphoma cells and Large cell of diffuse lymphoma and Large normal reactive cell.

Comparison	Small Diffuse Lymphoma Cells	Large Cell of Diffuse Lymphoma	Large Normal Reactive
T Test	8.0497E-266	6.17789E-25	
	Very High Significant		
Min	32	146	109
Max	698	917	800
Mean	346	521	280

Table 4. T test for comparing large cell diffuse lymphoma and the normal reactive cells.

Large	Mean Perimeter in Pixel	T Test	Mean Area in Pixel	T Test
Diffuse lymphoma 1	94	0.0	549	0.0
	Very high significant difference			
Diffuse lymphoma 2	88	0.0	536	0.0
	Very high significant difference			
Diffuse lymphoma 3	84	0.0	500	0.0
	Very high significant difference			
Diffuse lymphoma 4	93	0.0	620	0.0
	Very high significant difference			
Diffuse lymphoma 5	117	0.0	640	0.0
	Very high significant difference			
Reactive 2L	70		429	

Table 5. T test for comparing small cell diffuse lymphoma and the normal reactive cells.

Small	Mean Perimeter in Pixel	T Test	Mean Area in Pixel	T Test
Diffuse lymphoma 11	73	0.0	362	0.0
	Very high significant difference			
Diffuse lymphoma 12	75	0.0	389	0.0
	Very high significant difference			
Diffuse lymphoma 13	79	0.0	415	0.0
	Very high significant difference			
Diffuse lymphoma 14	71	0.0	317	0.0
	Very high significant difference			
Diffuse lymphoma 15	72	0.0	336	0.0
	Very high significant difference			
Reactive 2S	39		140	

ing variability could affect the optimum selection of the object to be identified by the program. To control color differences measures of density defined as RGB, such feature was examined in the preliminary study; leading to the selection of a range of RGB; used as a limiting parameter on starting the program. The range obtained was 121, 60, 116 minimum

Table 6. T-test comaring between Automatic and Manual cell extraction in Perimeter and Area in pixel on large cells.

Parameter		T test	
		Perimeter in Pixel	Area in Pixel
T test Result		0.2019	0.2722
T test		not significant	not significant
Automatic cell extraction mean		78	412
Range	Min	51	166
	Max	134	1157
Manual cell extraction Mean		82	445
Range	Min	49	153
	Max	134	1106

Table 7. T-test comaring between Automatic and Manual cell extraction in Perimeter and Area in pixel on small cells.

Parameter		T test	
		Perimeter in Pixel	Area in Pixel
T test Result		0.9242	0.8676
T Test		not significant	not significant
Automatic Mean		42	156
Range	Min	34	115
	Max	52	230
Manual Mean		46	157
Range	Min	35	110
	Max	58	220

RGB and 204, 100, 199 Maximum RGB; and the mean was 172, 85, 170. The selected RGB values were defined as maximum red, minimum green and maximum blue in pixels.

The material used in this study for validation of the technique consisted of normal lymph nodal tissue where the differentiation of lymphoid cells on the basis of size is clear; comparing large cells in germ centers and small cells in the interfollicular zone. The validation of the method was based on a preliminary study that relied on expert microscopist to define large from small cell populations.

The range of size for both large and small cells was measured in pixel value. The result helped in defining a threshold value (30 pixel) for the smallest object, meaning that any values below that threshold were excluded as being noise; further verified by the observer. The digital images dealt with in this research were characterized by the following features:

- Not fully connected contour.
- Frequent overlapped cells.
- Same color density of cytoplasm and background.
- Huge amount of data.

On completion of this sequence, the image related problems were corrected, as judged by expert observation. Whatever the method used in the field of digital microscopic im-

ages, researchers agreed on the importance of validation of the method used [11, 12].

In this research, sensitivity was ensured. Analysis of microscopic images of diffuse lymphoma aims at quantization of information in such a way that allows more objective interpretation and assessment of the data. Thus, cases of lymphoma could then be classified according to size. The categorization of mixed small and large cell lymphoma was not studied and will be the subject of further research. Our results point to accurate differentiation between lymphoid cell classes as being large or small.

Comparison of the mean (area in pixels) in cases of large lymphoma cells with reactive large lymphoid cells showed a significant difference. Comparison of the mean (area in pixels) in cases of small lymphoma with reactive small lymphoid cells also showed a significant difference.

CONCLUSION

Microscopic digital images of cases of lymphoid tissue whether of reactive or diffuse lymphomatous nature have been analyzed with the aim of identification of different cell populations based on the size using criteria of perimeter and area defined by pixels.

Image enhancement technique has been applied to improve the image quality by edge enhancement. Image segmentation for the purpose of facilitating automatic recording of the frequency of specific object (cells) repetition is applied.

The comparison between observations based on users selection of the object and automatic recording of comparable values was fulfilled. The system has been able to identify the small cell population from the large cells population under specified criteria of image processing and enhancement.

This paper presented a methodology to achieve a fully automated classification of Lymphoma cells from microscopic digital images. The methodology is based on the morphological analysis of cells. Results show that the presented methodology is achievable with remarkable classification accuracy. Further studies will be focused on enhanced adaptive segmentation modules, the impact on classification accuracy of enlarged sample dataset and the test of the overall system.

The system has been used for automatic identification of different cell population by fixing the RGB value and feeding the range of selected perimeter and area. It is ready for application in the medical field in cases of classification of lymphoma based on the cell size and on similar studies for evaluation and classification of hematologic malignances using bone marrow smears.

The main advantage of this proposed scheme over existing schemes is that, the developed system effectively identifies and classifies the images of Lymphoma containing multiple cells, while existing systems mostly consider only those images which have one cell under the field of view. This automated analysis assists pathologists in diagnosis and in lessening their time for reviewing large number of tissue slide per day and also reduces human error.

The system is able to identify the small cell population from the large cells population under specified criteria of image processing and enhancement. Sensitivity and specificity of the system have been reviewed by expert pathologists who agreed with system results. The system has been used for automatic identification of different cell population. He is one of the manuscript authors, Prof. Dr. Osama Hassan, an expert in this field and works as a consultant for a medical center of high-level service. The system is ready for application in the medical field in cases of classification of diffuse lymphoma based on the cell size.

FUTURE WORK

The system can be further developed for other applications on digital microscopic images.

Research in this field will be supported by medical imaging and pattern recognition and many of the computer assisted fields have more accurate programs. In image analysis, the segmentation techniques are varied. Image enhancement to any kind of cell features that extracted is changeable.

3D construction of tissue from this kind of images is difficult and therefore needs trials. Reaching a standard in this field is an important aspect and has not been achieved yet.

The system results detected to certain accuracy the intersection between large and small cell of lymphoma but needs enhancement. The availability of such systems can be of value in exchange of information both morphologically and morphometrically through Telepathology facilities. All these points of research described above still represent future challenges for the developed system.

The development of a fully automated screening system prototype for cell segmentation and classification may provide the specialist with significant aid in an effort to detect and classify lymphoma cells more effectively and efficiently.

CONFLICT OF INTEREST

The authors confirm that this article content has no conflict of interest.

ACKNOWLEDGEMENTS

I wish to thank Prof. Osama Hassan and Dr. Amr Al Sebaee from International Medical Center hospital for their profitable cooperation and encouragement, for providing the medical image data and interpretation for the analysis. Also their assistance is acknowledged in understanding the complete slide preparation procedure for histology image acquisition, being experts in histopathology and cytology.

REFERENCES

[1] LI H, ElMoataz A, Fadili J, Ruar S. An improved image segmentation approach based on level set and mathematical morphology. In Third International Symposium on Multispectral Image Processing and Pattern Recognition, International Society for Optics and Photonics 2003. p. 851-4.

[2] Huang K, Sharma A, Cooper L, Pan T, Gurcan M, Saltz J. A Novel Image Registration Pipeline for 3-D Reconstruction From Microscopy Images Department of Biomedical Informatics. Columbus 2007.

[3] Ar B, Anagha CK, Bharat R. Diagnostic Application of Mean Nuclear Area (MNA) Measured By Computerized Interactive Morphometry in Breast Cancer. J Pathol 2007; p. 5 (2).

[4] Junior JAP, Azoubel R, Martins AT, Maniglia JV. Value of Morphometry in the Prognosis of Laryngeal Neoplasms. Int J Morphol 2005; 23(3): p. 275-8.

[5] Baak JPA, Ørbo A, van Diest PJ, *et al.* Prospective Multicenter Multicenter Evaluation of the Morphometric D-Score for Prediction of the Outcome of Endometrial Hyperplasias. Am J Surgical Pathol 2001; 25(7): p. 930-5.

[6] Meijering E. Cell Segmentation: 50 Years Down the Road. IEEE Signal Process Mag 2012; 29(5): p. 140-5.

[7] Sandhya BS, Chayadevi M, Anitha P. Automated Classification of Centroblast Cells using Morphological and Texture Features. Int J Comput App 2013; 72(3).

[8] Han J, Ma KK. Rotation-invariant and scale-invariant Gabor features for texture image retrieval. Image Vis Comput 2007; 25(9): p. 1474-81.

[9] Paragios N. A level set approach for shape driven segmentation and tracking of the left ventricle. IEEE T Med Imaging 2003; 22(6): p. 773-6.

[10] Buhmeida A. Quantitative Pathology: Historical Background, Clinical Research and Application of Nuclear Morphometry and DNA Image Cytometry. Libyan J Med 2006; 1(2): p. 126.

[11] Jaakko L. Computer-Assisted Quantitative Image Analysis of Cell ProliferationAngiogenesis and Stromal Markers in Expermintal an Laryngel Tumor Development 2003.

[12] Yayun Z. Cell Segmentation Using Level Set Method. Johann Radon Institute for Computational and Applied Mathematics. 2007.

[13] Metin G, Tony P, Hiroyuki S, Joel S. Image Analysis for Neuroblastoma Classification: Hysteresis Thresholding for Nuclei Segmentation Department of Biomedical Informatics. The Ohio State University, ColuColumbus; Children's Hospital Los Angeles, Los Angeles, Calif. 2007.

[14] Korzynska A, Roszkowiak L, Lopez C, Bosch R, Witkowski L, Lejeune M. Validation of various adaptive threshold methods of segmentation applied to follicular lymphoma digital images stained with 3,3'-Diaminobenzidine&Haematoxylin. Diagn Pathol 2013; 8(48): p. 1596-8.

[15] D.Belsare, M.M M. Histopathological Image Analysis Using Image Processing Techniques: An Overview. Signal & Image Process Int J (SIPIJ) 2012; 3(4).

[16] Mashiah A, Wolach O, Sandbank J, Uziel O, Raanani P, Lahav M. Lymphoma and leukemia cells possess fractal dimensions that correlate with their biological features. Acta haematologica 2008; 119(3): p. 142-50.

[17] Howarth P, Yavlinsky A, Heesch D, Rüger S. Visual features for content-based medical image retrieval. In Proceedings of Cross Language Evaluation Forum (CLEF) Workshop; 2004.

[18] José dA. Advanced topics in image processing and analysis. Math Morphol 2004.

[19] Chen Q, Yang X, Petriu EM. Watershed Segmentation for Binary Images with Different Distance Transforms. In Proceedings of the 3rd IEEE Int Workshop on Haptic, Audio and Visual Environ App 2004; Ottawa, Ontario, Canada. p. 111-6.

[20] Prasad A,S, Latha K,S, Rao S,K. Separation and Counting of Blood cells using Geometrical Features and Distance Transformed Watershed. Int J Engin Inn Technol (IJEIT) 2013; 3(2).

[21] Rafael CG, Richard EW. Digital Image Process 2nd ed; 2002.

[22] Edward RD, Reberto AL. Hands-on Morphol Image Process SPIE. 2003.

[23] Unnati HBKT, Neil P. Human Ear Identification using Vector Quantization Algorithms. Int J Advanced Res Comput Commun Engin 2013; 2(12).

[24] Ramin S, Hossein R, Ardeshir T. Extraction of Nucleolus Candidate Zone in White Blood Cells of Peripheral Blood Smear Images Using Curvelet Transform. Comput Math Methods Med 2012; (12): p. 1-12.

[25] Monica M, Sos A, Anthony T,C. Deterministic model for Acute Myelogenous Leukemia classification. In IEEE International Conference on Systems Man and Cybernetics (SMC); 2012.

[26] Labati RD, Piuri V, Scotti F. The Acute Lymphoblastic Leukemia Image Database For Image Processing. In 18th IEEE international conference on Image processing (ICIP), 2011; 2012; Università degli Studi di Milano, Department of Information Technology, via Bramante65, 26013 Crema, Italy. p. 2045-8.

[27] Anna K, Lukasz R, Carlos L, Ramon B, Lukasz WML. Validation of various adaptive threshold methods of segmentation applied to follicular lymphoma digital images stained with 3,3'-Diaminobenzidine&Haematoxylin. Diag Pathol 2013; 8(48).

[28] Schäfer T, Schäfer H, Schmitz A, *et al.* Image database analysis of Hodgkin lymphoma. Comput Biol Chem 2013; 46: p. 1-7.

[29] Negm AES, Hassan OAF, Kandil AH. Segmentation of Blast Cells using K-means Clustering Technique. in press 2015.

[30] Menegaz G, Luti S, Duay V, Thiran JP. An interactive toolbox for atlas-based segmentation and coding of volumetric images. In International Society for Optics and Photonics 2007. p. 65124M-65124M-11.

[31] Polesel A, Ramponi G, Mathews V,J. Image enhancement via adaptive unsharp masking. Image Process, IEEE T 2000; 9(3): p. 505-10.

[32] Sonka M, Hlavac V, Boyle R. Image Process Anal Machine Vision, 2nd ed; 2014.

[33] Kesavamurthy T, SubhaRani S. Pattern Classification using imaging techniques for Infarct and Hemorrhage Identification in the Human Brain. Calicut Med J 2006; 4(3): p. e1.

[34] Cy C, Joanne W. Parallel Watershed Image Segmentation in Starp. In ; 2006.; http://www.interactivesupercomputing.com/success/downloads/Image Segmentation Presentation.pdf.

[35] Kekre H, Archana B, Patankar , Galiyal HR. Segmentation of Blast using Vector Quantization Technique. Int J Comput App 2013; 5(4).

[36] Fisher R, Perkins S, Walker A, Wolfart E. image processing learning resources. http://homepages.inf.ed.ac.uk/rbf/HIPR2/hipr_top.htm. 2003.

[37] Salihah AA, Mashor MY, Harun NH, Rosline H. Colour Image Enhancement Techniques for Acute Leukemia Blood Cell Morphological Features. In IEEE Intl Conf Systems Man Cyber 2010; p. 3677-82.

[38] Aimi SAN, Mashor M, Abdullah AA. Improving Blast Segmentation of Acute Myelogenous Leukemia (AML) Images Using Bright Stretching Technique. In Proceedings of the International Postgraduate Conference on Engineering (IPCE 2010); October 2010.; Perlis, Malaysia. p. 16-7.

[39] Pandey B, Mishra R. Knowledge and intelligent computing system in medicine. Comput Biol Med 2009; 39(3): p. 215-30.